Electronic Supplementary Material (ESI) for ChemComm.

Electronic Supporting Information

Phosphorylated-calix[4]arene-supported monometallic double-deckers of rare earth metal ions

Marjan Hosseinzadeh,*[a] Sergio Sanz,[b,c] Jan van Leusen,[a] Natalya V. Izarova,[a,b] Euan K. Brechin,*[d] Scott J. Dalgarno,*[e] and Paul Kögerler*[a,b,c]

Contents

General procedures. All reagents were used as received from commercial suppliers. Solvents were dried and degassed employing an MBraun SPS-800 solvent purification system. NMR experiments were recorded at 25 °C on a Bruker BioSpin 400 MHz NMR spectrometer equipped with a BBO Probe. Chemical shifts were referenced to the deuterated solvents themselves (^{13}C, ^{31}P) and reported relative to external $SiMe_4$ (^{1}H, ^{13}C) or 85% H_3PO_4 (^{31}P) standards. Electrospray mass spectra (ESI-MS) were obtained with the use of a Thermo Fisher Scientific LTQ Orbitrap XL mass spectrometer. Elemental analyses were performed by the Central Institute of Engineering and Analytics (ZEA-3), Forschungszentrum Jülich GmbH (52425, Jülich, Germany). UV-Vis experiments were performed in the range of 195–800 nm on a Shimadzu UV-2600 spectrophotometer using 10 mm quartz glass cuvettes. IR spectra were collected on a Bruker Vertex 70 FT-IR spectrometer on KBr disks. Thermogravimetric/differential thermal analysis (TGA/DTA) measurements were carried out with a Netzsch STA 409 C / CD in a dry N_2 flux (60 mL min^{-1}) at a heating rate of 5 K min^{-1}. Sets of Powder X-ray diffraction data were collected at room temperature with the aid of a STOE StadiP diffractometer (Stoe & Cie, Darmstadt, Germany; area detector; Cu Kα radiation; λ = 1.54059 Å).

Magnetic properties were determined using a Quantum Design MPMS-5XL SQUID magnetometer for direct current (dc) and alternating current (ac) measurements. Powdered samples of **2** and **3** were compacted and immobilised into cylindrical PTFE sample holders. Experimental dc data were recorded at 0.1 T and 1.0 T in the temperature range 2.0 – 290 K, and at 2.0 K in the field range 0 – 5.0 T. Experimental ac data were collected at various static bias fields between 0 and 2000 Oe in the temperature range 1.9 – 50 K and frequency range 3 – 937 Hz using an amplitude of B_{ac} = 3 G. However, **3** did not show relevant out-of-phase signals in this range. All data were corrected for the sample holder contributions and intrinsic diamagnetic contributions ($\chi_{m,dia}$ / 10^{-3} cm^3 mol^{-1} = –1.50 (**2**), –1.58 (**3**)). Single-crystal X-ray diffraction data for **1** – **3** were collected on a Bruker D8 Diffractometer operating with a Photon III detector at 100(2) K. Complexes **1** – **3** were revealed to be isostructural through unit cell comparison, but a full data collection was performed on **2**; crystals of **2** were found to be the most strongly diffracting, whilst those of **1**, in particular, turned out to be weakly diffracting. **Crystal data for 2 (CCDC 2085027):** $C_{123}H_{178}DyF_9O_{41}P_8S_3$, M = 2996.13 g/mol, triclinic, space group P-1 (no. 2), a = 16.141(4) Å, b = 24.753(6) Å, c = 25.146(7) Å, α = 77.616(7)°, β = 75.227(7)°, γ = 86.972(16)°, V = 9488(4) $Å^3$, Z = 2, T = 100.0 K, μ(CuKα) = 3.621 mm^{-1}, D_{calc} = 1.047 g cm^{-3}, 126160 reflections measured (3.654° ≤ 2Θ ≤ 118.348°), 27054 unique (R_{int} = 0.0998, R_{sigma} = 0.0907) which were used in all calculations. The final R_1 was 0.0844 ($I > 2\sigma(I)$) and wR_2 was 0.2608 (all data). Comments on crystallography: The structure has a reasonable degree of disorder. Whilst the majority of this could be modelled appropriately, it was necessary to apply a mask to deal with the third triflate anion that is disordered, but also resides on a special position. **Unit cell parameters for 1:** triclinic, a = 16.105(2), b = 24.676(3), c = 25.1001(3) Å, α = 76.847(6), β = 75.588(4), γ = 86.329(3)°. **Unit cell parameters for 3:** triclinic, a = 16.167(3), b = 24.6976(5), c = 25.1174(5) Å, α = 77.462(1), β = 74.983(1), γ = 87.356(1)°.

Synthesis and analytical characterisation. The precursor tetrakis-*O*-(diethoxyphosphoryl)-*p*-*tert*-butylcalix[4]arene (L_{PO}) was prepared according to the literature procedure.[1]

Synthesis of bis{tetrakis-*O*-(diethoxyphosphoryl)-*p*-*tert*-butylcalix[4]arene}yttrium(III) trifluoromethanesulfonate (1). A solution of yttrium(III) trifluoromethanesulfonate (0.0536 g, 0.10 mmol) and tetrakis-*O*-(diethoxyphosphoryl)-*p*-*tert*-butylcalix[4]arene (0.2386 g, 0.20 mmol) in 20 mL of acetonitrile was stirred overnight at ambient temperature. The reaction mixture was filtered to remove any unreacted species and the filtrate was then evaporated under reduced pressure to obtain

a white powder. Further purification of the product was achieved by crystallisation from $CHCl_3/Et_2O$. Yield: 0.2075 g (0.07 mmol, 71%).

^{1}H NMR (400 MHz, CD_3CN): δ 7.49 (s, 16H, Ar*H*), 4.98 (d, $^2J_{HH}$ = 16.0 Hz, 8H, CH_{2ax}), 4.44 (bs, 16H, POCH_2CH$_3$), 3.98 (bs, 16H, POCH_2CH$_3$), 3.67 (d, $^2J_{HH}$ = 16.0 Hz, 8H, CH_{2eq}), 1.40 (td, $^3J_{HH}$ = 7.0 Hz, $^4J_{HP}$ = 1.5 Hz, 48H, POCH$_2$CH_3), 1.27 (s, 72H, ^{t}Bu-CH_3) ppm; **^{31}P NMR** (162 MHz, CD_3CN): δ -15.04, -15.10 ppm; **^{13}C{^{1}H} NMR** (100 MHz, CD_3CN): δ 150.75 (d, $^5J_{CP}$ = 3 Hz, C_{ar}-para), 142.33 (d, $^2J_{CP}$ = 10.1 Hz, C_{ar}-OP), 133.34 (d, $^3J_{CP}$ = 2.9 Hz, C_{ar}-ortho), 126.93 (s, C_{ar}-meta), 67.47 (d, $^2J_{CP}$ = 6.8 Hz, POCH_2CH$_3$), 34.32 (s, C^{t}Bu), 31.03 (s, ArCH_2Ar), 30.44 (s, ^{t}Bu-CH_3), 15.39 (d, $^3J_{CP}$ = 9.4 Hz, POCH$_2$CH_3) ppm. **ESI$^+$ HRMS**, *m*/*z*: found 824.9936 $[M]^{3+}$ (100%), calculated for $[C_{120}H_{184}P_8O_{32}Y]^{3+}$: 824.9917; found 1311.9672 $[M + OTf]^{2+}$ (83% relative abundance), calculated for $[C_{121}H_{184}P_8O_{35}F_3SY]^{2+}$: 1311.9635. M = $[Y^{III}(L_{PO})_2]^{3+}$. **UV-Vis**, solution in CH_3CN, λ / nm (ε / 10^5 M^{-1} cm^{-1}): 200 (1.994), 270.5 (0.045), 279.5 (0.043). **IR**, KBr disk, ν / cm^{-1}: 2965 (s), 1291 (s), 1242 (s), 1188 (s), 1130 (m), 1031 (s), 1000 (s), 947 (m), 871 (w), 806 (m), 639 (m). **Elemental analysis**, calculated for $C_{123}H_{184}P_8O_{41}F_9S_3Y$: C 50.55, H 6.35%. Found: C 50.50, H 6.35%.

Synthesis of bis{tetrakis-*O*-(diethoxyphosphoryl)-*p*-*tert*-butylcalix[4]arene}dysprosium(III) trifluoromethanesulfonate (2). The same synthetic procedure used for $[Y^{III}(L_{PO})_2]$ $(OTf)_3$ (**1**) has been followed for the preparation of $[Dy^{III}(L_{PO})_2](OTf)_3$ (**2**), using $Dy(CF_3SO_3)_3$ in place of $Y(CF_3SO_3)_3$. Yield: 0.2217 g (0.07 mmol, 74%).

ESI$^+$ HRMS, *m*/*z*: found 849.6643 $[M]^{3+}$ (100%), calculated for $[C_{120}H_{184}P_8O_{32}Dy]^{3+}$: 849.6657; found 1348.9732 $[M + OTf]^{2+}$ (70% relative abundance), calculated for $[C_{121}H_{184}P_8O_{35}F_3SDy]^{2+}$: 1348.9749. M = $[Dy^{III}L_2]^{3+}$. **UV-Vis**, solution in CH_3CN, λ / nm (ε / 10^5 M^{-1} cm^{-1}): 200 (2.029), 271 (0.053), 279.5 (0.050). **IR**, KBr disk, ν / cm^{-1}: 2963 (m), 1480 (m), 1272 (s), 1240 (s), 1187(s), 1159 (m), 1126 (m), 1031 (s), 1000 (s), 894 (w), 870 (w), 806 (w), 638 (m). **Elemental analysis**, calculated for $C_{123}H_{184}P_8O_{41}F_9S_3Dy$: C 49.31, H 6.19%. Found: C 49.10, H 6.34%.

Synthesis of bis{tetrakis-*O*-(diethoxyphosphoryl)-*p*-*tert*-butylcalix[4]arene}terbium(III) trifluoromethanesulfonate (3). The same synthetic procedure used for $[Y^{III}(L_{PO})_2](OTf)_3$ (**1**) has been followed for the preparation of $[Tb^{III}(L_{PO})_2](OTf)_3$ (**3**), using $Tb(CF_3SO_3)_3$ in place of $Y(CF_3SO_3)_3$. Yield: 0.2095 g (0.07 mmol, 70%).

ESI$^+$ HRMS, *m*/*z*: found 848.3309 $[M]^{3+}$ (80%), calculated for $[C_{120}H_{184}P_8O_{32}Tb]^{3+}$: 848.3315; found 1346.9731 $[M + OTf]^{2+}$ (100% relative abundance), calculated for $[C_{121}H_{184}P_8O_{35}F_3STb]^{2+}$: 1346.9732. M = $[Tb^{III}L_2]^{3+}$. **UV-Vis**, solution in CH_3CN, λ / nm (ε / 10^5 M^{-1} cm^{-1}): 200 (2.122), 271 (0.053), 279.5 (0.051). **IR**, KBr disk, ν / cm^{-1}: 2964 (m), 1480 (m), 1272 (s), 1240 (s), 1187(s), 1159 (m), 1128 (m), 1031 (s), 1001 (s), 895 (w), 871 (w), 806 (w), 638 (m). **Elemental analysis**, calculated for $C_{123}H_{184}P_8O_{41}F_9S_3Tb$: C 49.36, H 6.20 %. Found: C 48.92, H 6.26%.

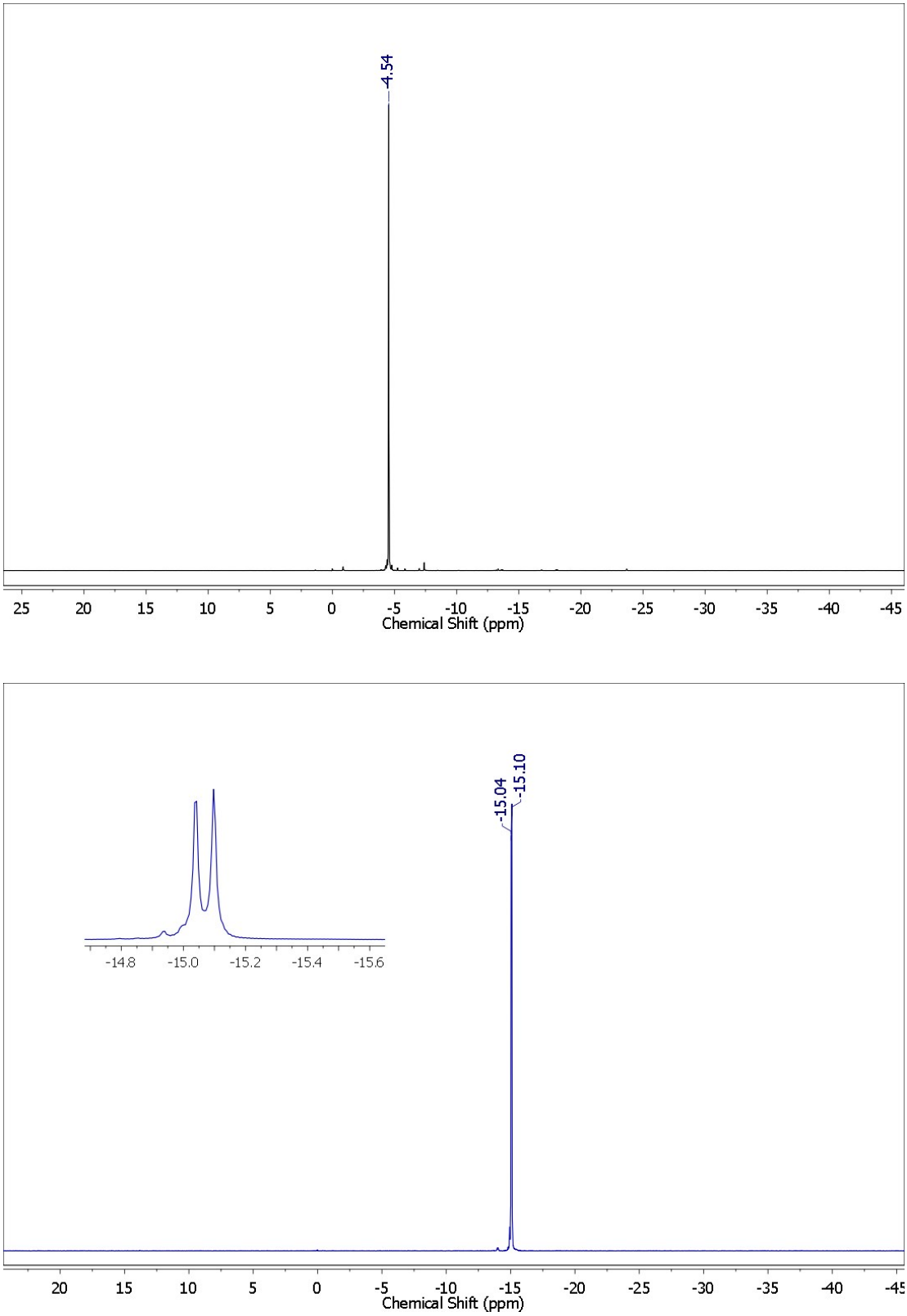

Figure S1. ^{31}P NMR (162 MHz, CD_3CN) spectra of the precursor tetrakis-*O*-(diethoxyphosphoryl)-*p*-*tert*-butylcalix[4]arene (L_{PO}) (**top**) and $[Y^{III}(L_{PO})_2](OTf)_3$ (**1**) (**bottom**).

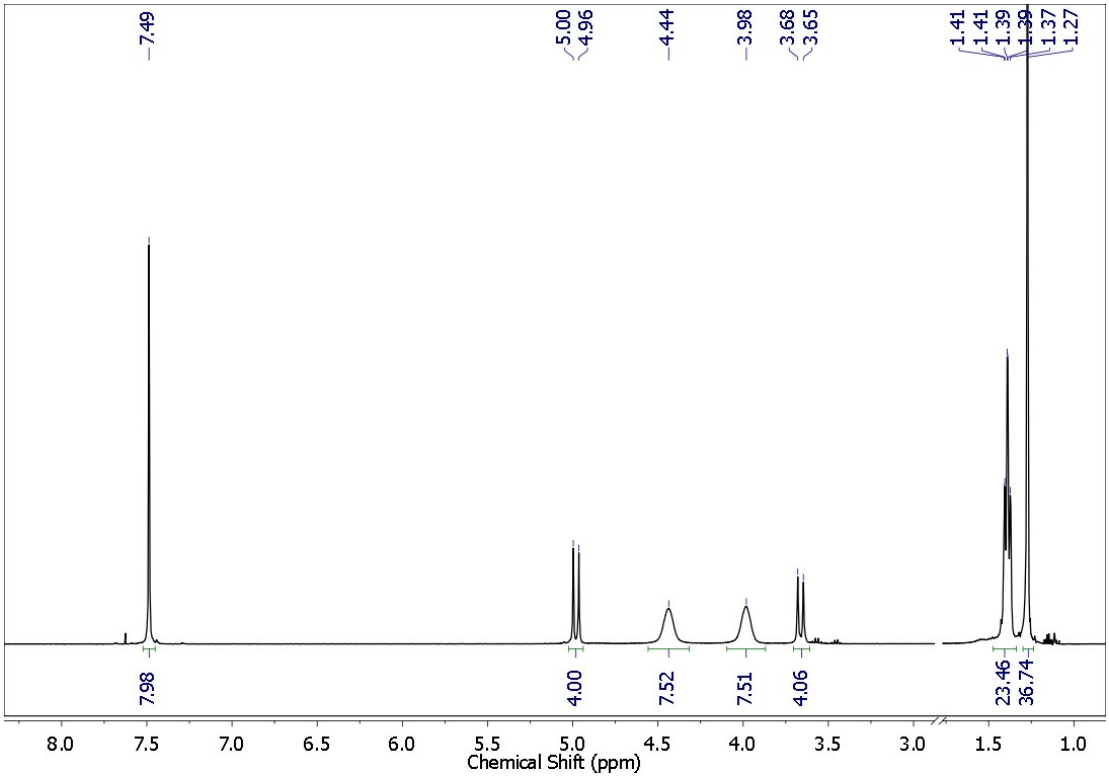

Figure S2. ^{1}H NMR (400 MHz, CD_3CN) spectrum of $[Y^{III}(L_{PO})_2](OTf)_3$ (**1**). Solvent signals have been removed for clarity.

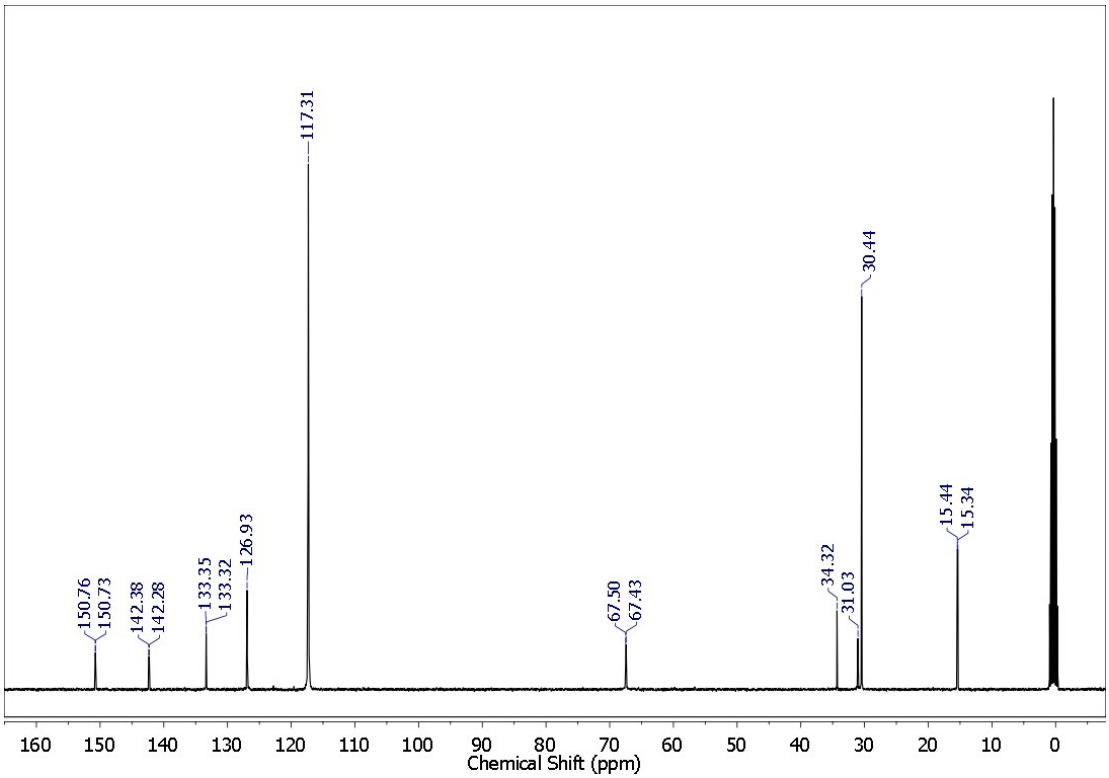

Figure S3. $^{13}C\{^{1}H\}$ NMR (100 MHz, CD_3CN) spectrum of $[Y^{III}(L_{PO})_2](OTf)_3$ (**1**).

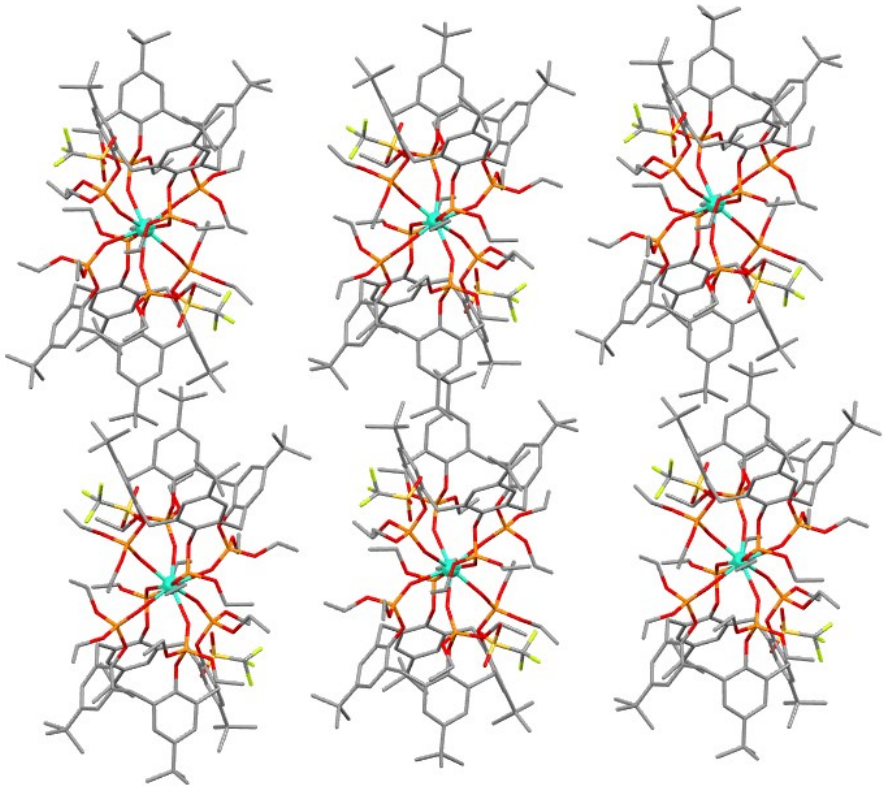

Figure S4. Extended molecule structure of **2** viewed along the *a* axis.

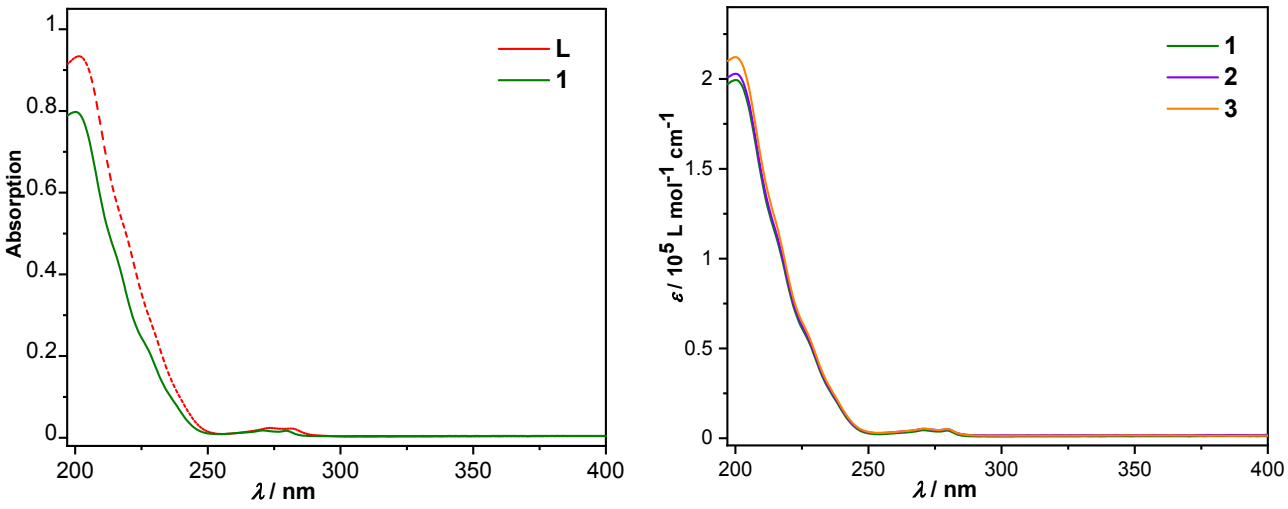

Figure S5. Left: UV/Vis spectra of CH_3CN solutions of $[Y^{III}(L_{PO})_2](OTf)_3$ (**1**) and the precursor tetrakis-*O*-(diethoxyphosphoryl)-*p*-*tert*-butylcalix[4]arene (L_{PO}). **Right**: Molar extinction graphs for $[Y^{III}(L_{PO})_2](OTf)_3$ (**1**), $[Dy^{III}(L_{PO})_2](OTf)_3$ (**2**) and $[Tb^{III}(L_{PO})_2](OTf)_3$ (**3**).

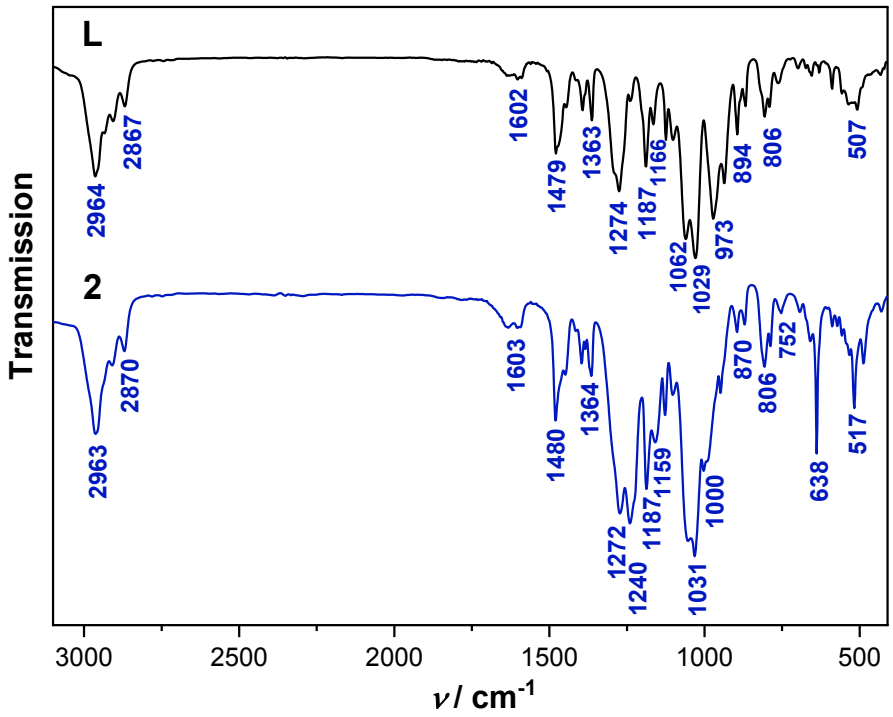

Figure S6. IR spectra of tetrakis-*O*-(diethoxyphosphoryl)-*p*-*tert*-butylcalix[4]arene (**L**, black graph) and $[Dy^{III}(L_{PO})_2](OTf)_3$ (**2**, blue graph).

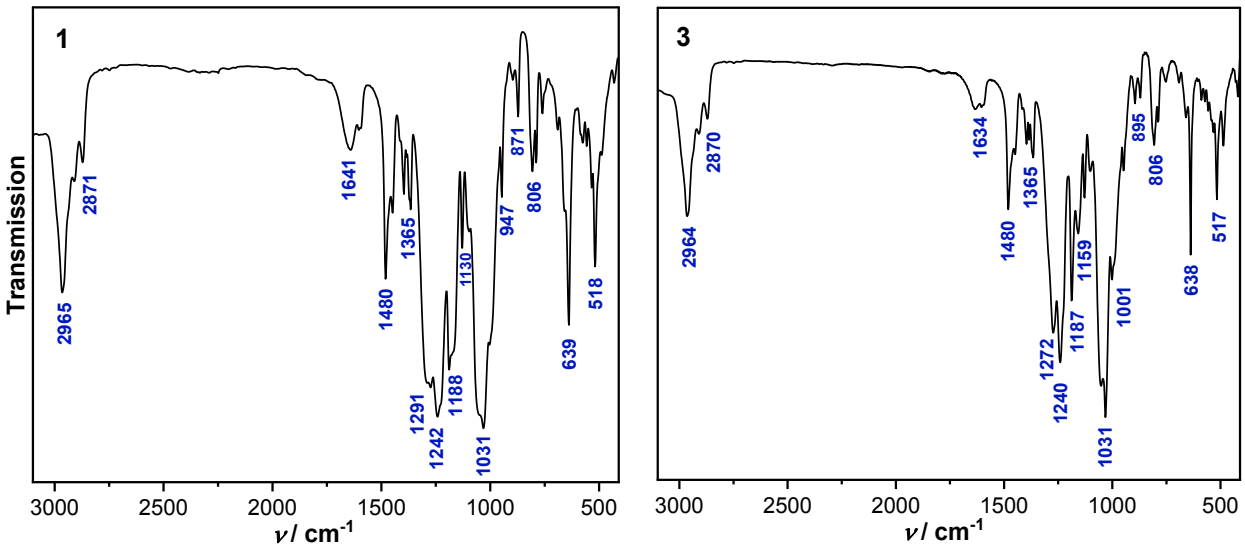

Figure S7. IR spectra of $[Y^{III}(L_{PO})_2](OTf)_3$ (**1**) (left) and $[Tb^{III}(L_{PO})_2](OTf)_3$ (**3**) (right).

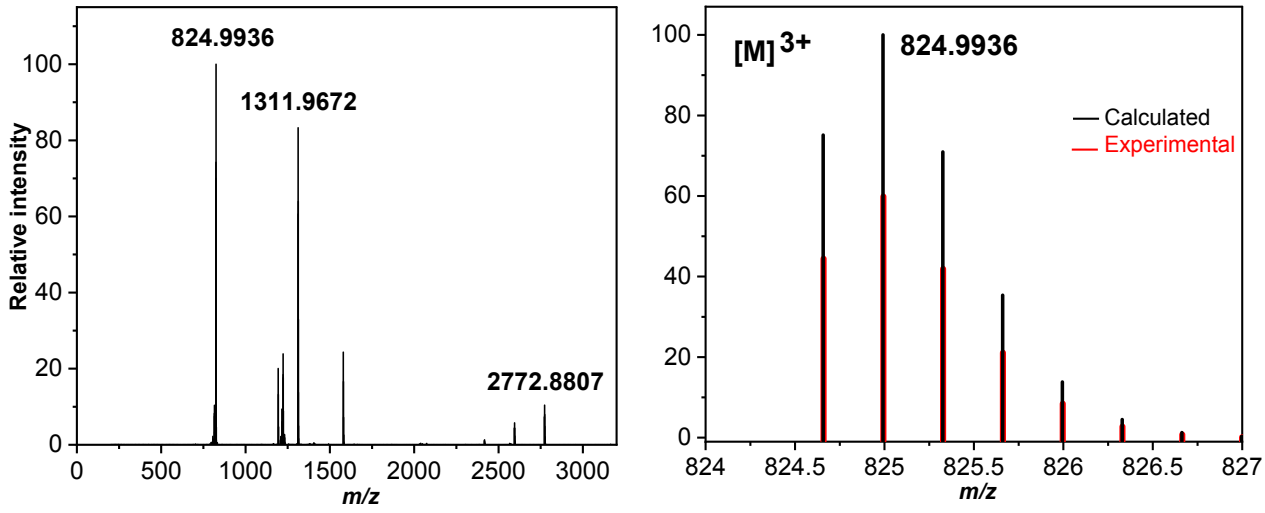

Figure S8. Left: Full ESI-HRMS spectrum of $[Y^{III}(L_{PO})_2](OTf)_3$ (**1**); *m/z*, found 824.9936 $[M]^{3+}$ (100% relative abundance), calculated for $[C_{120}H_{184}P_8O_{32}Y]^{3+}$: 824.9917; found 1311.9672 $[M + OTf]^{2+}$ (83%), calculated for $[C_{121}H_{184}P_8O_{35}F_3SY]^{2+}$: 1311.9635. **Right**: Partial ESI-HRMS corresponding to $[M]^{3+}$. M = $[Y^{III}(L_{PO})_2]^{3+}$.

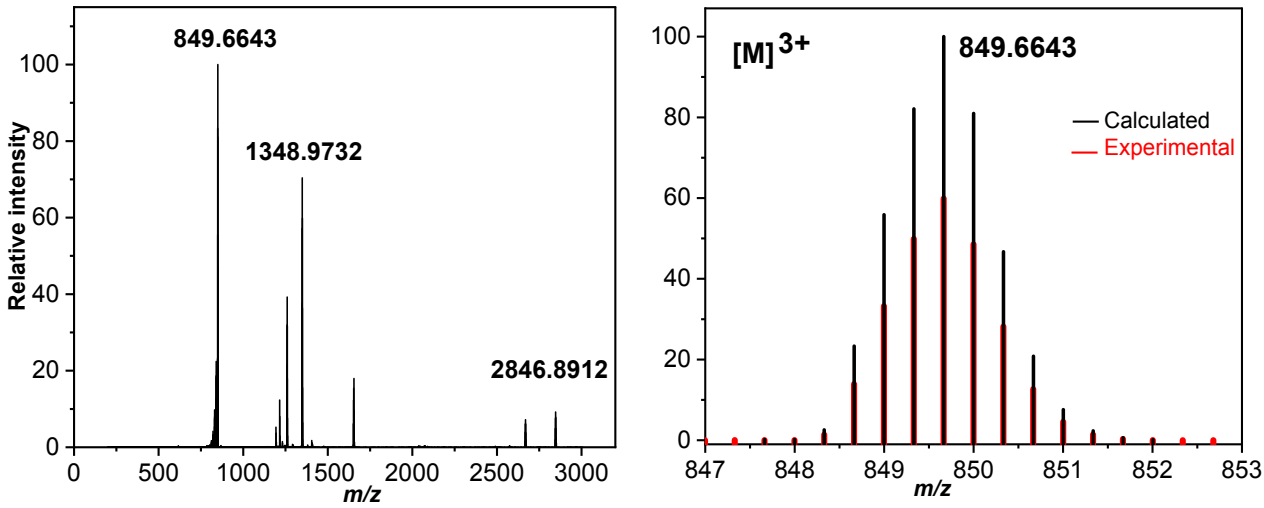

Figure S9. Left: Full ESI-HRMS spectrum of $[Dy^{III}(L_{PO})_2](OTf)_3$ (**2**); *m/z*, found 849.6643 $[M]^{3+}$ (100% relative abundance), calculated for $[C_{120}H_{184}P_8O_{32}Dy]^{3+}$: 849.6657; found 1348.9732 $[M + OTf]^{2+}$ (70%), calculated for $[C_{121}H_{184}P_8O_{35}F_3SDy]^{2+}$: 1348.9749. **Right**: Partial ESI-HRMS corresponding to $[M]^{3+}$. M = $[Dy^{III}(L_{PO})_2]^{3+}$.

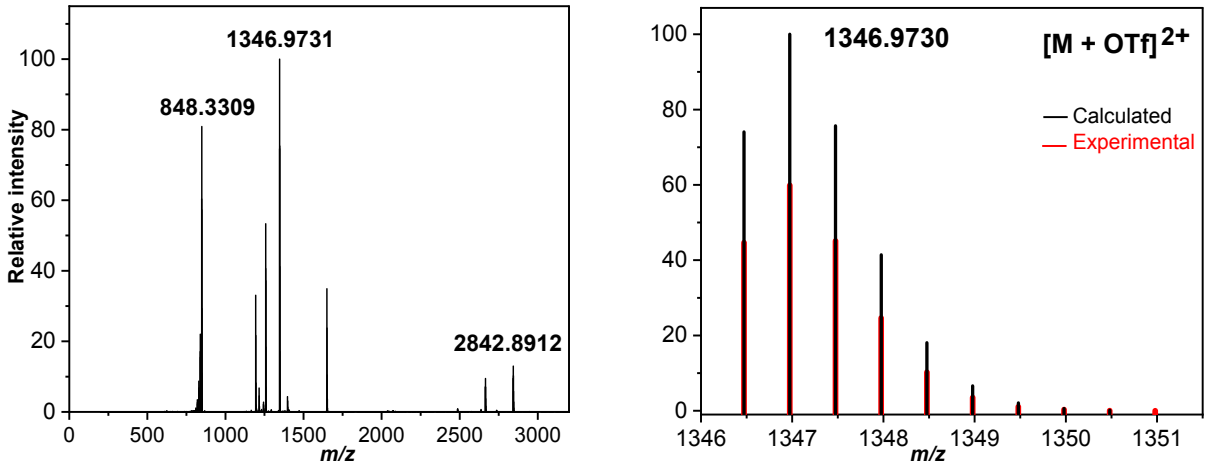

Figure S10. Left: Full ESI-HRMS spectrum of $[Tb^{III}(L_{PO})_2](OTf)_3$ (**3**); *m/z*, found 848.3309 $[M]^{3+}$ (80% relative abundance), calculated for $[C_{120}H_{184}P_8O_{32}Tb]^{3+}$: 848.3315; found 1346.9731 $[M + OTf]^{2+}$ (100%), calculated for $[C_{121}H_{184}P_8O_{35}F_3STb]^{2+}$: 1346.9732. **Right**: Partial ESI-HRMS corresponding to $[M + OTf]^{2+}$. M = $[Tb^{III}(L_{PO})_2]^{3+}$.

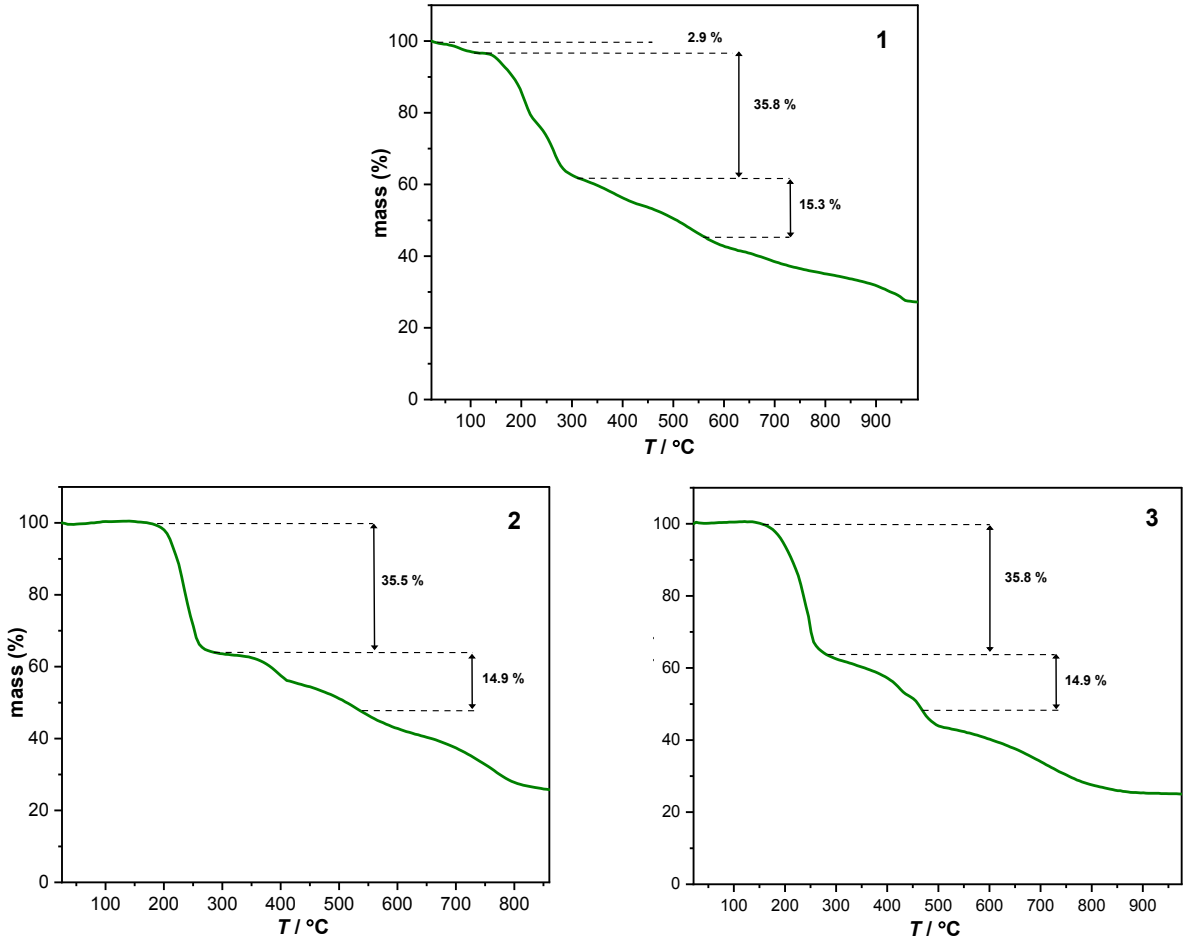

Figure S11. Thermogravimetric analysis (TGA) of **1** (**top**) **2** (**bottom left**) and **3** (**bottom right**). All compounds exhibit significant thermal stability up to approximately 200 °C. The mass loss of until ~500 °C may correspond to the loss of three triflate units.

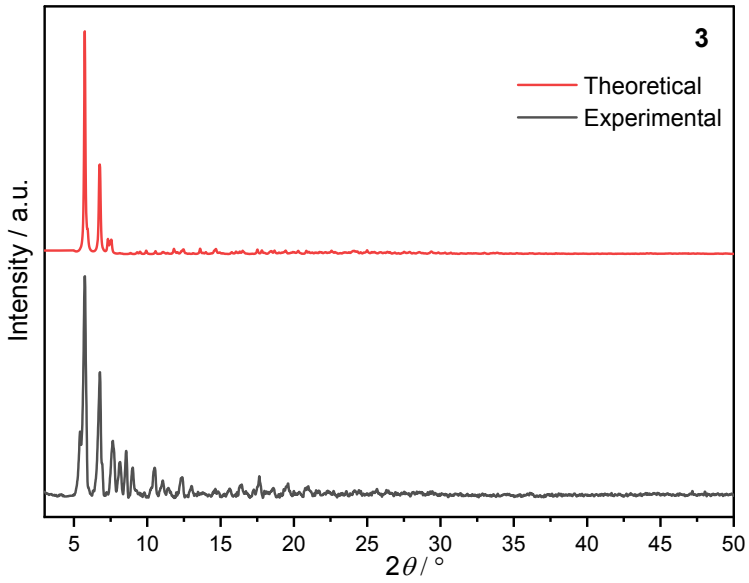

Figure S12. Experimental powder X-ray diffraction (PXRD) pattern of **3** as representative for compounds **1** – **3** measured at room temperature (bottom) and theoretical PXRD pattern (top) calculated from single-crystal X-ray diffraction data. We observe a partial loss of crystallinity in samples **1**–**3** over the course of the measurements due to rapid loss of crystallisation solvent causing the appearance of additional weak signals vs. the simulated PXRD pattern.

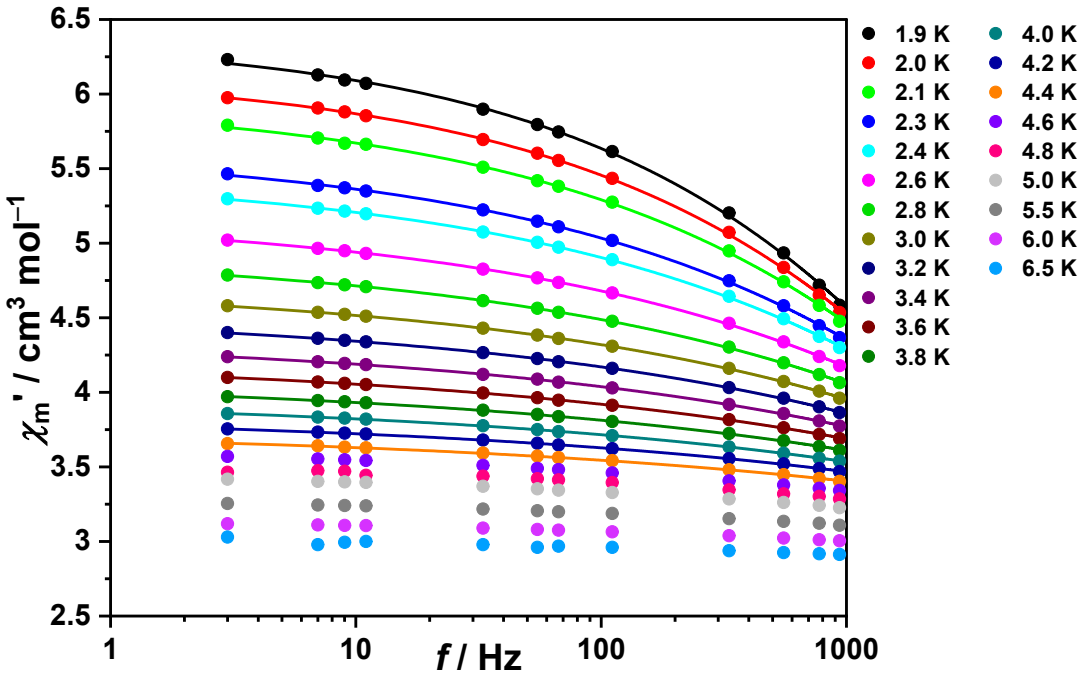

Figure S13. In-phase χ_m' *vs.* frequency *f* plots of **2** at a static bias field of 500 Oe (circles: data, lines: least-squares fits).

References

1. Z. Goren and S. E. Biali, *J. Chem. Soc. Perkin Trans.*, 1990, 1484–1487.